surfaces

MDPI

Article

Study on the Lubrication Performance of Graphene-Based Polyphosphate Lubricants in High-Temperature Steel–Steel Friction Pair

Kaifu Mi [1], Qingqing Ding [2], Xiangru Xu [1], Yu Lei [1], Juncheng Wang [1] and Ning Kong [2,*]

[1] Beijing Petroleum Machinery Co., Ltd., Beijing 102206, China; mikfdr@cnpc.com.cn (K.M.); xuxrdr@cnpc.com.cn (X.X.); leiyudr@cnpc.com.cn (Y.L.); wangjcdr@cnpc.com.cn (J.W.)
[2] School of Mechanical Engineering, University of Science and Technology Beijing, Beijing 100083, China; m202220565@xs.ustb.edu.cn
* Correspondence: kongning@ustb.edu.cn

Abstract: In the study, a hybrid lubricant was prepared by introducing graphene into a polyphosphate lubricant. In the tribological test of a steel/steel friction pair at the high temperature of 800 °C, the addition of a small proportion of graphene significantly enhances the lubrication performance of polyphosphate at elevated temperatures. The coefficient of friction and the wear were obviously held down while the surface quality of the high-temperature friction pair was enhanced effectively with the graphene-strengthened polyphosphate lubricant, compared with the dry sliding condition. Through scanning electron microscopy and Raman spectroscopy analysis, the formation mechanism of tribofilm and the antiwear performance of the hybrid lubricant are further explained. This lubricant effectively combines the advantages of both; the combination of polyphosphate melted at elevated temperature with graphene and metal surfaces ensures the self-sealing of the friction contact area and brings better high-temperature oxidation resistance. At the same time, the presence of graphene provides excellent strength to the friction film and ensures the anti-wear and wear-resistant performance of the lubricant at high temperatures.

Keywords: graphene; polyphosphate; tribofilm; lubricant; elevated temperature

Citation: Mi, K.; Ding, Q.; Xu, X.; Lei, Y.; Wang, J.; Kong, N. Study on the Lubrication Performance of Graphene-Based Polyphosphate Lubricants in High-Temperature Steel–Steel Friction Pair. *Surfaces* **2024**, *7*, 571–588. https://doi.org/10.3390/surfaces7030039

Academic Editor: Aleksey Yerokhin

Received: 14 June 2024
Revised: 26 July 2024
Accepted: 7 August 2024
Published: 11 August 2024

1. Introduction

With the rapid development of industrial production, the upgrading of mechanical production equipment and the continuous deepening of development environments have brought about more demanding working conditions and more extreme application scenarios. The use of lubricants to reduce working friction, improve the service life of rolling mills, enhance the surface quality of steel, and increase economic benefits in the field of the hot rolling of steel [1,2] has always been a long-term research topic. The working temperature of hot rolling is generally between 800 and 1100 °C, and traditional lubricants may cause serious environmental problems due to by-products and lubricant residues under extreme high temperature conditions. Therefore, the design of lubricants with good wear reduction performance, strong wear resistance and durability, good high-temperature resistance, and environmental protection requirements [3–5] is increasingly attracting the attention of scholars.

Carbon-based nanomaterials are widely used in the field of tribology due to their stable chemical properties, excellent mechanical properties, and tribological properties. Carbon-based nanomaterials have different shapes. There are carbon-based materials with different shapes including fullerene, carbon nanotubes, graphene, nanodiamond, and graphite. They can be suitable for different lubrication needs and become a composite lubricant. Compared with other carbon-based nanomaterials, graphene has high mechanical strength. As an additive, it can adapt to various complex-use environments. At the same time,

graphene is almost not corroded by other solvents and can be mixed with many liquids and solids to improve the lubricating properties of mixed lubricants. Li M. [6] effectively enhanced the lubrication performance of the friction oil film in the milling area during TC4 alloy processing by adding graphene to vegetable oil. Wang W. et al. [7] used graphene and ethyl orthosilicate as raw materials to prepare composite lubricating materials in the ball. In the ball–disc friction experiment, the wear rate was reduced by a minimum of 61.7%. Ibrahim et al. [8] used graphene as an additive in palm oil, and the friction coefficient and cutting energy consumption were significantly reduced compared with commercial lubricants. The use of graphene-based lubricant preparation benefits from the excellent properties of graphene materials. The preparation and lubrication performance research of graphene-based lubricants has become one of the research directions in the field of tribology.

However, relevant research shows that under extreme friction conditions, the graphene crystal structure will be damaged, and the damaged graphene will break into graphene fragments [9], making it difficult to continue to function. However, when intact original graphene sheets are used as lubricating additives, it is inevitable that due to their complete structure, it is difficult to spread evenly in the solvent, and it is easy to produce irreversible agglomeration, which makes it impossible to cover the surface under friction conditions during actual work [10,11], and take advantage of its anti-wear properties. At the same time, due to the characteristics of carbon-based materials, graphene undergoes graphitization as the temperature increases above 100 °C, so the characteristics of preheated graphene [12] are the same as those of graphite at high temperatures. The reason for this phenomenon is that the representative Hummers method [13,14] commonly uses inorganic strong proton acid (concentrated sulfuric acid or nitric acid or both of them) to deal with the original graphite, meaning intercalating the strong acid molecules between the graphite layers, then oxidizing it with strong oxidizer (potassium perchlorate, potassium permanganate, etc.). The hydroxyl, carboxyl, ether is inserted between graphite layers to expand the layer spacing through oxidation; thus, graphite is stripped into single-layer or multilayer graphene oxide, and finally, graphene is obtained via chemical reduction. If this type of graphene had a high temperature treatment, it would be easy to graphitize (high temperature makes groups between the layers condense into water and then evaporate, resulting in graphene layer spacing shrinking). Graphitization here is a negative result due to some of the excellent properties of graphene disappearing, which is a major problem to overcome when graphene is used as a high-temperature lubricant.

Inorganic polyphosphate glass polymers are considered potential materials for lubricant additives with outstanding physical and chemical properties in temperature engineering applications. They assume a molten fluid state at high temperatures and can enhance lubricant capture and delivery to friction contact areas. It can effectively reduce the friction coefficient [15] and effectively protect the oxidation of the metal substrate. At the same time, the wear resistance of polyphosphate at high temperatures [16] is an insurmountable problem. There are related research surfaces; for example, through a nanoparticle-enhanced minimum quantity lubrication (MQL) technique, a small amount of nanoparticle input is not only limited to save resources, but also the formation of a lubricating film has good performance, significantly reducing the temperature on the contact surface of the workpiece [17], obtaining a good surface finish. The mechanism of nano-lubrication is extraordinarily complex, but a reasonable proportion of the additive and the control of preparation conditions are expected to make nanometer lubrication achieve a zero wear rate and self-repair. The addition of graphene can strengthen polyphosphate and oxide nanopowers [18], potentially improving their wear resistance.

In conclusion, both graphene and polyphosphate are considered effective lubrication additives in the field of high-temperature lubrication, and both have their own limitations. So, in this study, we can combine the advantages of both to produce a hybrid material based on sodium polyphosphate and graphene using ultrasonic oscillation [19]. Based on actual high-temperature transmission (bearings, gears, etc.) and hot-rolling working conditions,

we have selected a typical steel/steel friction pair. Contrast tribological testing in elevated temperature (800 °C) steel/steel friction pair aimed to emphasize the huge potential of the hybrid lubricant to markedly reduce friction and wear and enhance the surface quality [20] of friction pair. Microscopic inspection of damaged surfaces of disks and balls can elucidate the lubrication mechanism of auxiliary materials at high temperatures.

2. Experimental Section

2.1. Preparation of Hybrid Lubricants

In the current investigation, hybrid lubricants were prepared into three types [21], employing a facile synthesis route. The first kind of lubricant called G-PO (abbreviation of graphene prepared by physical method, polyphosphate, and oxide) mainly consists of a proper amount of commercially available graphene nanoplatelets (thickness of 1 nm, concentration of 1 mg/mL) and three types of commercially available sodium polyphosphate ($Na_4P_2O_7$,$(NaPO_3)_6$,Na_5P_3O10). In addition, oxide nanoparticles (Al_2O_3 (30 nm), TiO_2 (40 nm), and SiO_2 (50 nm)) were added as a supplement between graphene layers, and a small amount of organics also joined in G-PO to strengthen the dispersion of graphene in water. While the second called PO (short for polyphosphate and oxide) does not contain graphene compared with G-PO, the third kind of lubricant (logogram as G) was only made from graphene nanoplatelets identical with G-PO. All of the three were rapidly mixed using a blender for 12 h in the wake of being continuously sonicated in deionized water for 2.5 h to guarantee the full mixing of several kinds of materials and graphene loosing into a single layer or a few layers. As observed in Figure 1, G-PO finally formed a stably dispersed opaque gray suspension; PO corresponded to the white, and G was naturally black just like graphene nanoplatelets. All preparations served the assessment of significant role of trace graphene and nanoparticles maintaining the excellent performance of graphene.

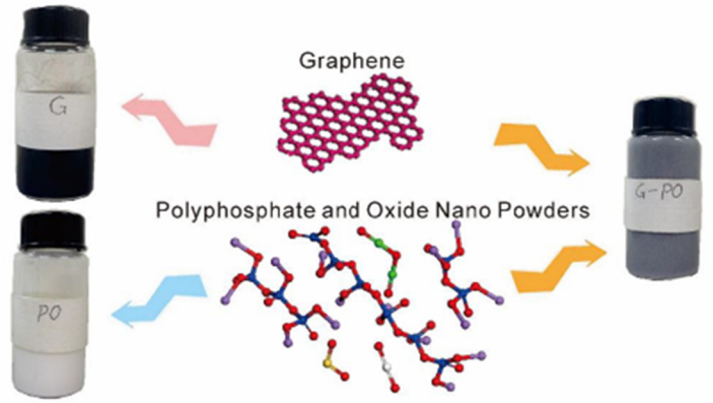

Figure 1. Three formulated lubricants and their main components.

2.2. Thermogravimetric Analysis (TGA)

In order to apply graphene to a high-temperature lubrication field, the thermal stability should be inspected firstly, using thermogravimetric analysis (TGA) with temperatures ranging from room temperature (about 25 °C) to 1000 °C at a rate of 10 °C/s. TGA was carried out on the three kinds of powder, respectively, coming from the three kinds of lubricants dried first, in both dynamic air and nitrogen atmosphere. In consideration of the high-temperature condition, the lubricants weighed accurately were loaded into platinum crucibles with a diameter of 4 mm cleaned in hydrochloric acid previously. During the thermogravimetric analysis, sample weight was measured using a thermobalance, and the change value along with the temperature was recorded by means of analysis software for the TGA system. After TGA, the samples were not taken out until cooling down from 300 °C.

2.3. Friction Characteristics of Hybrid Lubricants at High Temperature

In order to have a preliminary assessment of the prepared lubricant, friction coefficient measurements were performed [22] in air at 800 °C using the CSM-THT01-04015 tribometer with a ball-on-disk contact geometry in sliding mode, and the temperature regime is shown in Figure 2. The steel flat samples (GH150) of 30 mm diameter and the counterpart steel ball (GCr15) of 6 mm diameter were initially cleaned in the ultrasonic cleaning machine soaked in ethanol to clear away all of the organic impurities which may have been left after the machining and thermal treatment operations performed as sample preparation. The original arithmetical mean deviation of the profile of both the disk and the ball samples was Ra = 0.1 µm. The experimental environment temperature is 25 °C and the relative humidity is 45%. As shown in Figure 2, during the tribotests, the counterpart steel ball runs in circle with a radius of 4 mm on the steel flat at a speed of 190 rpm (or 8 cm/s), and the normal load is 10 N (average Hertz contact stress is 1.402 GPa). The sliding test duration of each pair of ball and flat was 20 min or 3800 cycles (100 m). The friction was performed for steel–steel contact using lubricants prepared previously, and the lubricants were supplied in about 0.2 mL volumes in the contact areas before the rotation of the disk, and periodically in drops (3 drops or 0.15 mL of solution) every 2 min along with the rotation to make sure the lubricants present in the wear track. The friction coefficient measured using the recorder along with the tribotests represents variations in friction resistance in the direction of travel, whereas roughness measured using a 3D measuring laser microscope after the experiments represents the geometry of the surface. Each friction test is repeated three times to ensure the accuracy and objectivity of the experimental data.

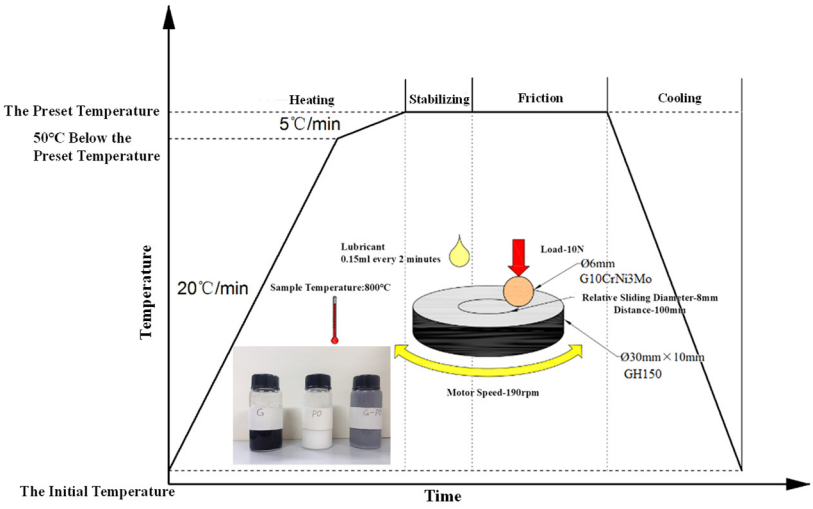

Figure 2. The temperature regime and the conditions of the tribotests.

2.3.1. High-Temperature Friction Test Materials

The metal sample is divided into an upper test ball and a lower test disk. Both metal samples are purchased uniformly. The test ball is made of GCr15, a type of carburized bearing steel. This type of steel has good hardenability and can achieve uniform strength over a large cross-sectional range. The sample hardness is 341 HB, and the tensile strength can reach 980 MPa, with good comprehensive mechanical properties, good machinability, and moderate cold deformation plastic parts and weldability. Gears, bearings, shafts, worms, bolts, pins, etc. are used for working under high load conditions. The test disk is made of GH150 material, which is a precipitation-strengthened Ni Fe-based high-temperature alloy. The mechanical properties of GH150 are very outstanding, with a tensile strength of over 1250 MPa at room temperature and a hardness of 230 HB. Although the strength decreases slightly at high temperatures around 700 °C, it still maintains a tensile strength of around 950 MPa. In addition, the alloy also has excellent durability and creep performance.

2.3.2. Setting of Friction Experiment Parameters

There are many factors that affect friction, but in friction experiments, the parameter conditions that can be changed are limited, mainly including load, time, temperature, speed, original roughness of the friction interface, sample size and material, and lubrication conditions. The setting of these parameters needs to be determined based on the actual application conditions and the reaction characteristics of the material.

(1) Test load

Referring to the contact stress between general mechanical transmission components (standard involute spur cylindrical gear teeth), it is mostly below 1000 MPa. Therefore, setting the load to 1000 MPa or above in the experiment meets the working requirements of most gear transmission components. The formula for calculating Hertz contact stress [23] in ball disc contact is as follows (1):

$$\sigma_H = 0.388\sqrt[3]{\frac{PE^2}{R^2}} \quad (1)$$

σ_H—H Hertz contact stress, Pa;

P—Load, N;

E—Elastic modulus, taken as 206×10^9 Pa;

R—Test ball radius, taken as 3×10^{-3} m.

If σ_H is taken as 1000 MPa, P = 3.63 N can be calculated. Here we take a load of 10 N and substitute it into Formula (1) to calculate the reverse value of $\sigma_H = 1402 \times 10^6$ Pa = 1402 MPa.

(2) Speed

The setting of the rotational speed refers to the relative sliding speed between the rolling mill and the rolled piece during the hot rolling process, which is generally considered to be around 5% to 10% of the rolling speed. Based on the F1 frame of a hot rolling mill in a certain factory, the rolling speed is about 1.4 m/s. Therefore, the relative sliding speed between the rolling mill and the rolled piece is about 0.07–0.14 m/s. Taking into account various conditions, the set speed for this experiment is 0.08 m/s (with a relative sliding diameter of 8 mm, the corresponding speed is 190 rpm).

(3) Temperature

The recrystallization temperature of steel is approximately within the range of 900 °C to 990 °C. However, if the experimental temperature is set within this temperature range, deformation will have a complex impact on the shape of the sample, making it difficult for later detection. Moreover, during the hot working process, it is generally not possible for both friction interfaces to be above this temperature. Friction experiments require heating the ball and disk samples to the set temperature, so it is reasonable to choose a relatively low temperature for simulating actual friction, with high temperatures of 700 °C and 800 °C. Meanwhile, 650–850 °C is the temperature range with the richest products in high-temperature reaction research and is an important temperature node. Comparative experiments were conducted under four conditions, dry friction, G-lubrication, PO lubrication, and G-PO lubrication, at 700 °C and 800 °C.

2.3.3. High-Temperature Friction Test Equipment

(1) Scanning electron microscope (SEM)

The SUPRA 55(ZEISS Germany) field emission scanning electron microscope (SEM) was used to observe the wear marks on the surface of the ball and disk samples after the 800 °C high-temperature friction experiment. Scanning electron microscopy uses a point-by-point imaging method to convert the surface features of the sample into image signals in order and proportion.

(2) Raman spectrometer

By using high-temperature Raman spectroscopy for in situ detection at several important temperature nodes, a more comprehensive study of the reactions and products throughout the entire temperature range can be conducted, which is of great significance

for ultimately revealing the dynamic lubrication mechanism of lubricants with temperature changes. This article uses the high-temperature hot stage of the LabRAMHREvolution(HORIBA FRANCE France) high-resolution Raman spectrometer (Raman Spectrometer) for this experiment. The laser emission wavelength is 532 nm and the output power is 50 mW. Raman spectroscopy typically measures the Stokes scattering of scattered light relative to the frequency reduction in incident light to determine the class of scattering molecules, and the frequency difference between the scattered light and incident light is the Raman shift.

3. Results and Discussion

3.1. Thermogravimetric Analysis (TGA) Results

The TGA result of the G lubricant shows that the two curves fell slowly in the same way around 200 °C, and in dynamic nitrogen, graphene remained losing weight slowly until 1000 °C (the end of the experimental temperature), yet in dynamic air, the oxidation rate of graphene increased at around 400 °C, slowed down at 500 °C, but began to rise sharply at 600 °C, and the total gravimetric lost at 800 °C is shown in Figure 3a. Graphene undergoes surface decomposition or combustion at 400 °C, and undergoes severe oxidation between 600 °C and 800 °C, accompanied by a clear exothermic peak, producing CO or CO_2 that flows out with the incoming gas. Therefore, the G lubricant has difficulty surviving under aerobic conditions above 800 °C. The thermogravimetric curve of graphite in air is very consistent with the curve measured in this analysis. In addition, the condensation of functional groups between layers causes more layers of graphene to aggregate and bond more tightly, resulting in graphitization. Therefore, at a specific temperature, graphene transforms into graphite, exhibiting typical characteristics of graphite and losing some of its better properties.

One of the purposes of adding polyphosphate and oxide nanopowder is to inhibit graphitization; the thermal stability of polyphosphate and oxide nanopowder ought to be investigated in advance. Take a look at the TGA curves of PO lubricant; it is evident from Figure 3b that the thermal stability of PO is good no matter in the air or nitrogen. Although the weight dropped with the increase in temperature a little, that might be due to the vaporization of organics after the temperature reached their boiling points, at which point they have completed the mission when the water evaporates. By this token, polyphosphate and oxide nanopowder are likely to play a positive role to improve the overall thermal stability of the hybrid lubricant G-PO.

The thermal stability of G-PO containing all the active ingredients is the focus. The curves of G-PO are shown in Figure 3c; there is no big gap between the TGA curves of G-PO and PO in general, and both the initial weights (about 11.7 mg vs. 12.3 mg) and the final weight losses (about 2.5 mg vs. 2.5 mg) of the two samples have not much difference. In addition, the colors of the G-PO samples which were removed as soon as the temperature reached 800 °C to compare with pure graphene are still various degrees of gray; namely, the color was lighter in air, darker in nitrogen. It suggests that polyphosphate and oxide nanopowder make a contribution to restrain graphene from burning out at least under 800 °C.

The insert in each image is the SEM image of the initial appearance of the lubricating film at room temperature. On the one hand, these images represent the original microstructure of each sample before heating up, affecting the friction characteristics [24], and on the other hand, they provide an image reference for looking for an approximate structure after tribotests at high temperature.

Under anaerobic condition, three kinds of lubricant powder have excellent thermal stability, and also, graphene existing below 800 °C, when the application conditions turn into contact with oxygen, can still play a strong role; the thermal stability of the other two components is also top-ranking. The samples of G-PO are gray at 800 °C, which suggests that the favorable interaction of hybrid materials in the study cannot be underestimated. Since the melting points of oxide nanopowder added are relatively high, phosphate is in a

partly molten state at more than 600 °C, just at which graphene starts burning in air. So that graphene and oxide nanopowder can be wrapped in molten phosphate, graphene is prevented from burning out to a certain extent. During the friction experiments or friction in actual production, in addition to the package action of phosphate, the space between the relatively closed friction pair also cut off part of the air. Based on the above research, graphene is likely to exist above 600 °C, even 800 °C. It is concluded that the temperature of the friction test is 800 °C.

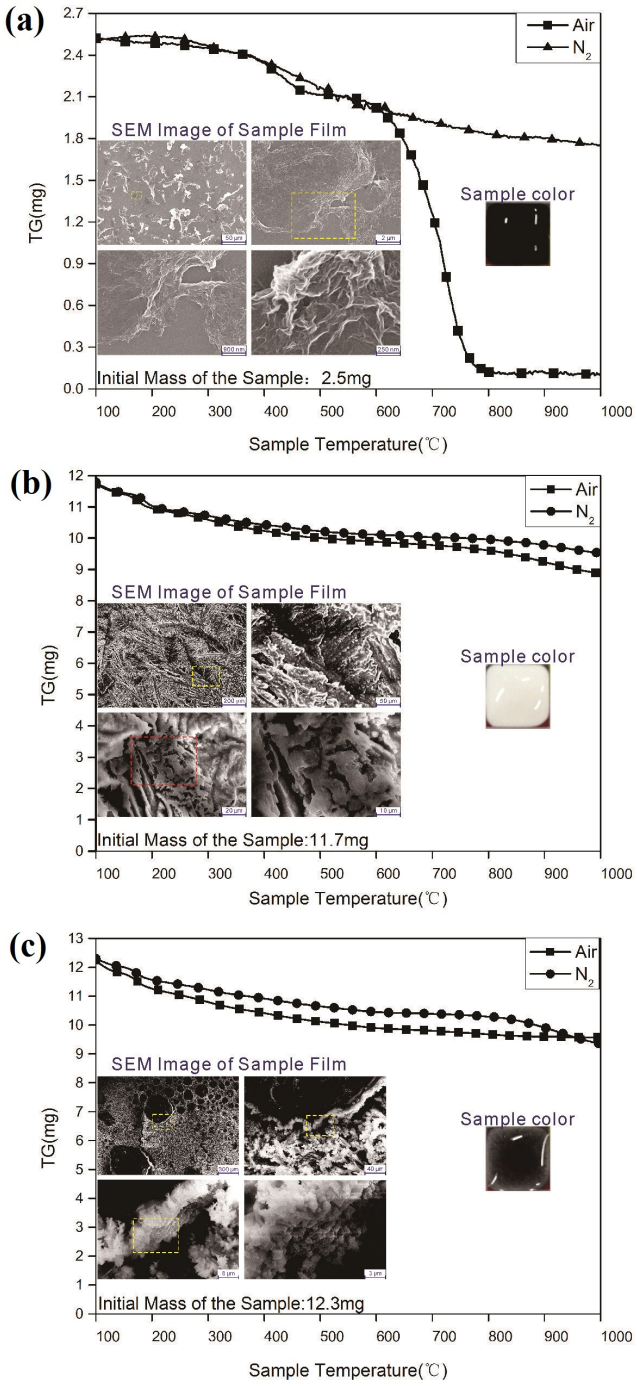

Figure 3. The TG curves and SEM images of (**a**) G showing its thermal stability in air and N2 and micro-morphology of initial film; (**b**) PO showing its thermal stability in air and N2 and micro-morphology of initial film; (**c**) G-PO showing its thermal stability in air and N2 and micro-morphology of initial film.

3.2. Assessment of Lubrication Performance of Hybrid Materials

To investigate the effect of the nanoscale hybrid materials on the friction and wear of sliding steel test pairs at elevated temperature, a benchmark test for the same 3800 cycles with various lubricated friction was carried out with bare steel in air under a 10 N load at 800 °C [25]. Subsequently, we performed a number of experiments with three distinct lubricants: G, PO, and G-PO, prepared previously. And during the tribotests, the regular supply of lubricants was necessary to guarantee that the correlative lubricant remained present in the grinding crack throughout the friction period. As shown in Figure 4, under dry friction conditions, the two friction interfaces cannot be separated due to the lack of lubricant, resulting in direct contact. The actual contact area is large, and the shear resistance of the metal interface is high. In addition, the plowed debris cannot be carried out by lubricant, resulting in a large frictional resistance. The friction coefficient is around 0.8, and the wide curve indicates that the stick slip motion is very significant. The adhesive force between the metal interfaces at high temperatures is large, directly increasing the shear resistance. The small fluctuation amplitude and short period of the curve indicate that although the friction conditions are harsh, the friction is stable without the addition of other media.

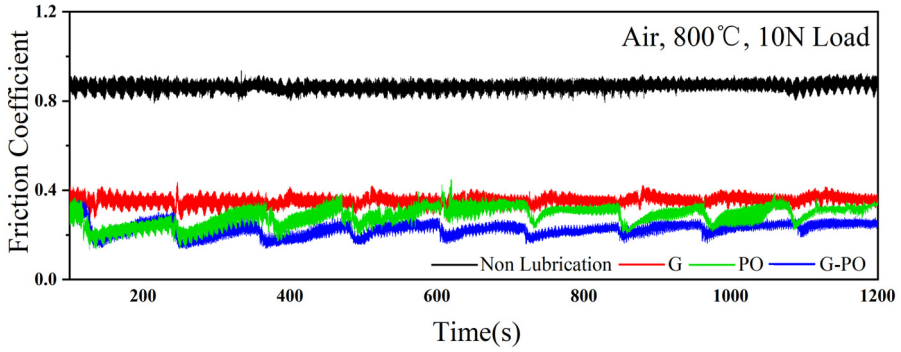

Figure 4. Friction coefficient vs. time curves of dry friction and tribotests under different lubrication conditions.

The curves under each lubrication condition exhibit varying degrees of periodic fluctuations of approximately 120 s, due to the addition of lubricant every 2 min during the friction experiment. At each time point of dripping, there will be a slight decrease in the friction coefficient, and within each 2-min cycle, there will be a slight increase in the friction coefficient. This indicates that if the lubricant is consumed under high temperature conditions, the decrease in lubricant composition will cause an increase in friction resistance. If the supply amount is more sufficient or the supply cycle is shortened, the wear reduction effect will be better.

The friction coefficient for the test performed in the G lubricant was reduced to 0.36 and remained stable in the first 10 min. This friction coefficient reduction is thought to be due to the lubrication of flakes of layered graphene during sliding and the relatively tight initial graphene film formed on the disk before rotation. The significance of keeping the graphene layer can be seen from Figure 4. After 10 min (around 1900 cycles), the average value of the friction coefficient for the steel interfaces with graphene as the lubricant increases a little, and the cyclical fluctuations (2 min as a cycle) in the coefficient of friction increases as well. The short life span of the initial graphene layer is blamed on the weak adhesion of graphene with the steel surface under extreme conditions. The poor adhesion of graphene itself at high temperature as well as the disappearance of the initial graphene film leads to the deterioration of the lubrication effect. Nevertheless, the peak value of volatility in the friction coefficient for the steel interfaces covered with graphene is much lower than the coefficient of friction for bare steel, explaining that graphene can effectively reduce the friction coefficient as a high temperature lubricant. In this case, the initial graphene layer during sliding was squeezed quickly out of the wear scar, resulting in a high friction

coefficient. There is thereby an urgent need, though it is still an importance challenge, to prolong the lifetime of the initial graphene layer by adding other ingredients.

Then, the lower curve of the friction coefficient, attained by periodically adding drops of PO into the sliding interface, indicates that the friction coefficient directly presents 2-min cycle fluctuations without a relatively stable stage. Although the amplitude is larger, the average value of the friction coefficient for the test performed in the PO lubricant is 0.24, lower than in the G lubricant. This interesting phenomenon indicates that alkali metal polyphosphate compounds have an admirable chemical affinity to the steel surface, fully ensuring a strong adherence to the melting polyphosphate film to the steel surface; however, polyphosphate and oxide nanopowders have worse strength. Every time after adding drops of PO, phosphate and oxide nanopowders formed an effective lubricant film at once, which is more favorable for antifriction and antiwear and inhibition of steel surface oxidation than graphene, but the film was soon worn out at 800 °C, and then the film debris was massively pushed outside of the wear track. Consequently, the contact areas of the friction pair started to suffer increasing steel-to-steel contact, resulting in more abrasive wear. The weak high temperature wear resistance of phosphate and oxide nanopowders is expected to improve by adding graphene with high tensile strength.

For the last data set, G-PO was supplied to the wear track periodically. As it can be clearly seen from Figure 4, the test reduced the friction coefficient to around 0.18 and the low friction values can be preserved for quite a long time in a fairly stable mode. This friction reduction can be attributed to the interaction of graphene and the hybrid of phosphate and oxide nanopowders. The stable frictional behavior needs to give its credit to the appropriate supplement of the lubricant; this is not because of the shortened supply period, but the prolonged effective time of the lubricant. The period of dropping the G-PO can precisely guarantee the formation of a steady tribolayer and make sure the tribolayer does not to lose efficacy. The lubricant film composed of G-PO is capable of maintaining an outstanding role in 2 min (about 380 cycles). Thus, the procedure of adding G-PO periodically showed to be remarkable even until 3800 cycles (the test was stopped after 3800 cycles) without obvious changes in friction performance. Such friction behaviors allow us to identify that the strong adhesion of phosphate in a molten state effectively confined graphene between friction interfaces to protect it from being pushed out, and, in return, coated graphene strengthened the lubricating film composed of phosphate and nanopowder, then this strengthening effect extends the effective time of the lubricant. Graphene and the hybrid of phosphate and nanopowder work together in the contact area, avoiding the adverse effect of the respective and combining the advantages of both.

The comparison of the friction coefficients clearly verifies the antifriction effect of the above three lubricants, and this is consistent with the result previously expected. To further explore their tribological properties, we will discuss the impact on wear [26] next. Two indicators were selected to evaluate the effect of each lubricant on reducing wear: the roughness at grinding mark on the disks and the calculated wear of the disks and balls included.

As shown in Figure 5, the wear of the disks is characterized by 3D topography and the height profile of grinding marks on steel plates is measured using OLYMPUS LEXT OLS4000 3D laser confocal microscopy(OLYMPUS Japan). The 3D topography shows the microscopic surface morphology at the grinding marks and their vicinity (red color corresponds to the highest point where a convex peak is present, blue to the lowest point where a sunken valley is present) after the sliding. The roughness values are calculated according to the height data of the height profiles, aiming at comparing the degree of wear and tear of the steel plates on several different lubricating conditions in more exact numerical values. As shown in Figure 5a, the root mean square roughness reaches up to 18.926 μm (there is a wide and deep sag in height profile, the max width of the grinding mark is 2.419 mm), and the wear damage on the plate develops to a very serious level (the gap between the highest and lowest regions reaches about 55 μm in the 3D topography, and large green areas indicate a great deal of material loss). For the test in the G lubricant,

although the range of wear is narrow (the max width is about 1.410 mm), a lot of ups and downs are shown in the grinding mark (Rq = 14.159 μm, and the height range is about 40 μm from −20 μm to 20 μm) in Figure 5b. Figure 5c shows the wear pattern of the steel plate with PO lubricant. Almost as bad as dry friction, not only is the width of grinding mark as high as 1.994 mm but the range of the height also reaches up to about 80 μm, higher than dry friction. The result of the sliding test with G-PO shown in Figure 5d is included in what we are mainly concerned with. Firstly, the edge of the grinding mark formed after sliding with G-PO is smooth in comparison to other lubrication conditions based on laser micro-images. Though the width is almost as large as the wear scar after dry friction, the roughness value is quite small (Rq = 8.099 μm, the height range is about 25 μm from −10 μm to 15 μm). Graphene is very effective in narrowing the wear width, but a dramatical reduction in wear of the steel plate requires the coverage of the lubricating film formed together with polyphosphate, oxide nanoparticles, and graphene. And it is precisely the relatively large width of grinding mark formed under the action of G-PO so that the friction coefficient and roughness exhibit a visible reduction at 800 °C, which is because the broad and shallow wear scars can contribute to low and steady friction coefficients [27] and smooth height profiles of materials by reducing and distributing the contact stress evenly.

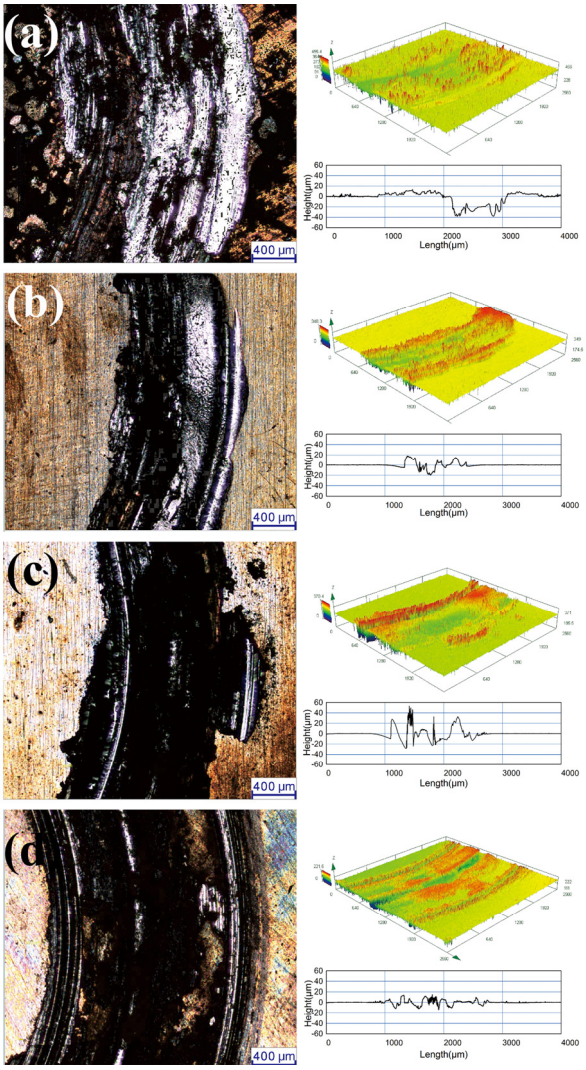

Figure 5. Laser scanning confocal microscopy, 3D topography, and height profile of the grinding mark for (**a**) dry friction; (**b**) tribotest under G lubricant; (**c**) tribotest under PO lubricant; (**d**) tribotest under G-PO lubricant.

The proof of the wear of the ball is wear volume, related to the wear diameter of the steel ball. We used the following equation to estimate the wear volume for the balls:

$$V_1 = (\frac{\pi h}{6})(\frac{3d^2}{4} + h^2) \quad (2)$$

$$h = \frac{D - \sqrt{D^2 - d^2}}{2} \quad (3)$$

In the formula,
V_1—Wear volume of the steel ball, mm^3;
h—Height of worn area, mm;
D—Grinding mark diameter, mm;
d—Diameter of the test ball, mm.

The wear width of the steel plate can be obtained through preliminary observation under a microscope, and its wear amount can be calculated using Formula (4). The wear amount of the steel plate can be approximately calculated by taking samples at equal intervals, which is equivalent to accumulating the volumes of a finite number of rings with different radii and heights but the same width. The starting and ending points of the accumulation are the positions where the wear marks enter and exit on the radius, respectively. The actual calculation of the height of each point took the average of the heights at the four equal points, but due to the highly uneven surface morphology in the wear marks, the calculation still has a large error. Here, only a rough comparison is made.

$$V_2 = \sum_{i=1}^{n} \Delta x \cdot y_i \cdot 2\pi x_i \quad (4)$$

In the formula,
V_2—Wear volume of the rigid disc, mm^3;
Δx—The distance between the radial sampling points (0.25×10^{-3})mm;
y_i—Radial position of sampling point, mm;
x_i—Height of sampling point, mm.

The calculations of disk and ball wear volume are shown in Table 1 and Figure 6. The estimate of disk wear is the accumulation of each ring wear volume in the direction of radius in the grinding mark of the disk. Both disk and ball volume calculations give expression to the striking antiwear property of each lubricant, especially G and G-PO, whose common ingredient is graphene. Graphene itself has very high tensile strength, causing it to be able to keep its original size in a single layer, which makes G play a very excellent antiwear role. The antiwear effect of G is slightly higher than that of G-PO, which may be due to the difference in the amount of graphene.

Table 1. Disk and ball wear volume calculations for 3800 cycle tests at 10 N load at 800 °C.

Test Conditions	Wear Diameter of Ball (m)	Wear Volume of Ball (m^3)	Wear Rate of Ball (Pa^{-1})	Wear Volume of Disk (m^3)
Non-Lubrication	2.193×10^{-3}	3.956×10^{-10}	3.960×10^{-13}	9.083×10^{-10}
With G	1.387×10^{-3}	0.617×10^{-10}	0.620×10^{-13}	2.330×10^{-10}
With PO	1.750×10^{-3}	1.542×10^{-10}	1.540×10^{-13}	5.423×10^{-10}
With G-PO	1.974×10^{-3}	2.580×10^{-10}	2.580×10^{-13}	2.579×10^{-10}

Based on friction coefficients and wear volumes, it is apparent that even a small amount of G-PO reduces the friction and wear of the steel ball and disk substantially at elevated temperatures, even for the long duration tests up to 3800 cycles. If we think that the high antifriction capacity of polyphosphate and oxide nanoparticles can be concluded by comparing the friction coefficient, graphene has better abrasion resistance [28] and can be extracted according to the comparison of wear volume. These results suggest that

polyphosphate reinforced by graphene combined with oxide nanopowders could be an excellent semimolten lubricant for extreme environments.

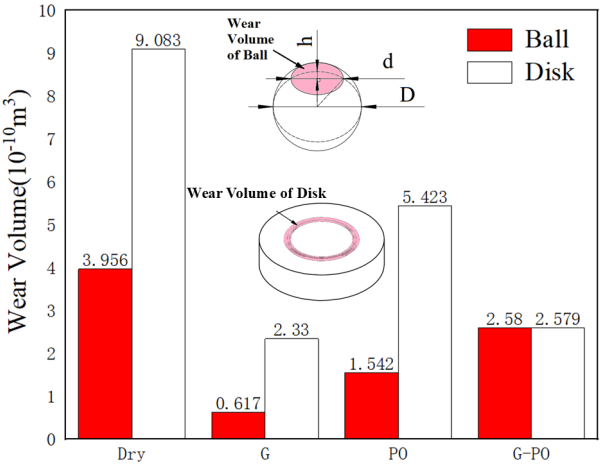

Figure 6. Wear loss of steel/steel pair under unlubricated and different lubricated conditions at 800 °C.

3.3. The Microstructure of Friction Surfaces and Lubricant in Wear Tracks

In order to elucidate the mechanism of the strengthening action of graphene to polyphosphate at rubbing steel/steel contacts at 800 °C, an observation of wear track on the plate and wear scar on the ball using a scanning electron micrograph (SEM) confirms the state of the contact area after sliding in Figure 7, where it shows striking contrasts of the wear situations in different lubrication conditions. Figure 7a,b are, respectively, ball and plate without lubrication. Terrible surfaces and obscure edges are easily caught sight of, and damage in both is exacerbated by the dual action of dry friction at high temperature and thick oxide formed during the test. Figure 7c,d represent a typical situation under the lubrication of G, where the edge of the grinding mark of plate is not very smooth, but very narrow, and the wear diameter of ball is quite small, which explains fully that graphene has a good abrasion resistance. By comparison, PO's antiwear property is not so ideal in view of the fact shown in Figure 7e,f, that the steel matrix and oxide around wear marks on the ball flake off, and the grinding mark on the plate is as wide as that for dry friction. Figure 7g,h show large-sized, but smooth and delicate grinding cracks on both the ball and plate under the lubrication of G-PO. In the actual industrial production, as little as possible or shallow or flat wear marks like Figure 7d,h are expected to minimize the impact on machine operations.

This further enlargement of the grinding marks on plates shown in Figure 8 directly show that the introduction of lubricant into high-temperature steel/steel friction pairs has the function of inhibiting the surface oxidation of the contact zone in addition to the anti-wear and antifriction action at 800 °C. Figure 8a shows the morphology of a large amount of slaggy iron oxide formed under dry friction conditions, representing a very serious oxidation condition. Figure 8b–d exhibit the presence of different amounts of acicular iron oxides after tests under various lubrication conditions. As described in the relevant literature, alkali metal salts play a positive role in improving anti-oxidation stability in the high temperature as lubricant additives [29], which is confirmed by our comparative observations. As shown in Figure 8c,d, acicular iron oxides are sparse and mixed with other particles (probably crystalline polyphosphate and oxide nanoparticles); however, acicular iron oxides are dense and widespread in Figure 8b under the condition lubricated only by graphene. Therefore, the phosphate film in molten state provides not only the viscous lubricant additive but also outstanding resistance to oxidation as predicted.

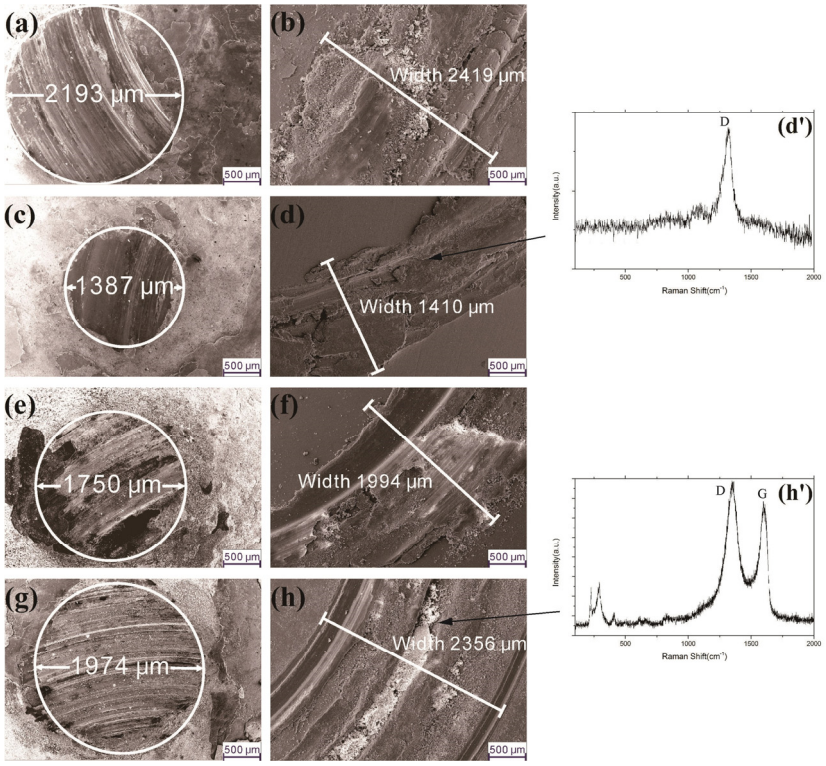

Figure 7. SEM images of wear scars and tracks on the ball and flats after tribotests without lubricants (**a**,**b**), with G (**c**,**d**), with PO (**e**,**f**), and with G-PO (**g**,**h**); the Raman spectra of points within the grinding tracks on the flats after tribotests with G (**d′**) and G-PO (**h′**).

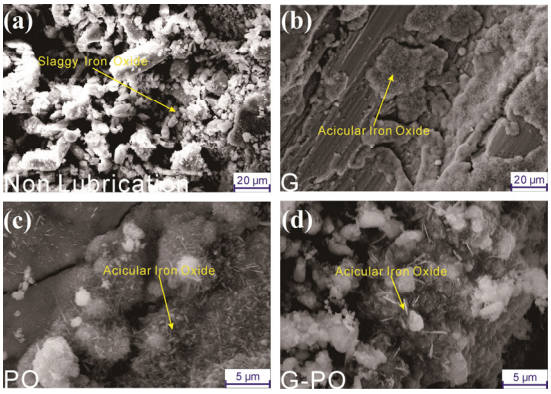

Figure 8. Iron oxides in the grinding marks on the plates formed during tests at 800 °C without lubricants (**a**); with G (**b**); with PO (**c**); and with G-PO (**d**).

As mentioned above, melting polyphosphate film has a strong adherence to the steel surface, and maybe it also has good adhesion to graphene. Raman spectroscopy via LabRAMHREvolution is used to determine whether the presence of graphene could be attributed to the action of molten polyphosphates [30], confirmed by the Raman spectra (shown in Figure 7d′,h′). For the test with the G lubricant, after the test was finished, the G peak is missing and the D peak (related to single phonon and defects) intensity detected everywhere on the wear scar on plate is low in Figure 7d′. The phenomenon shows that Raman spectroscopy cannot detect the graphene under such conditions, showing that either graphene hardly exists or the density of graphene is too low to be detected via Raman spectroscopy (The magnification of Raman spectrometer is about 500×). However, the disappearance of graphene does not indicate that graphene does not act as a lubricant in high-temperature friction. For the case of G-PO, the graphene has been damaged with

grinding marks after the sliding tests, shown in Figure 7h′. The intensity of D and G peaks with good signals in the wear scar is appreciable, and the presence of the D peak (at 1350 cm^{-1}) indicates that graphene is defected, destroyed by tribological interfaces [31], causing the friction coefficient to increase slightly. The weak peaks at around 700 cm^{-1} in both Figure 7d′,h′ represent iron oxides. The peaks at around 300 cm^{-1} in Figure 7h′ are the signal for the other ingredients of the G-PO lubricant. These finding indicate that graphene can hardly stay for a while by itself, but can persist for a long time after polyphosphate was added. The interaction between graphene and polyphosphate needs to be further explained in their mechanism. The following study targets the wear mark on the plate produced under the lubrication of G-PO.

The gradually enlarged SEM images (Figures 9 and 10) of the wear tracks of the plate in the case of G-PO indicate the retained form of graphene. A color-consistent dashed frame represents an enlarged image of a series in Figure 9, so (b) is the detail image of (a), and (c) and (e) are two details of different positions in (b), (d) is a further amplification of (c) and (f) is for (e). In Figure 9b, both the blue and red dashed frames are on the interior of the grinding mark. In Figure 9c emerges a sieve plane, but in Figure 9d with the highest magnification, the sieve "plane" is proved to be composed of uniform particles that are compared with the microscopic structure in inserts of Figure 3, confirmed to be oxide nanoparticles bound together with polyphosphate. The particles in Figure 9f have a clear lamellar structure, which could include graphene. And its size is micron, consistent with the graphene raw material for the preparation of lubricants.

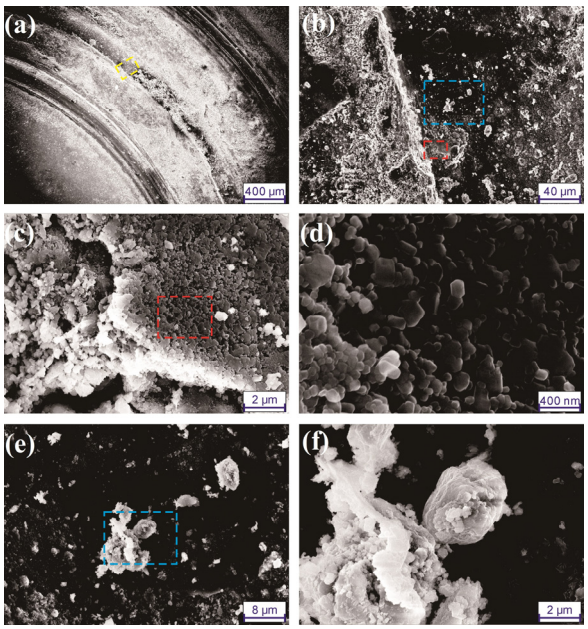

Figure 9. The gradually enlarged SEM images of the interior of the grinding mark after tribotest with G-PO: (**a**) SEM image of the grinding mark; (**b**) the detail image of (**a**); (**c**) the detail image of the red position in (**b**); (**e**) the detail image of the blue position in (**b**); (**d**) The further amplification image of (**c**) and (**f**) the further amplification image of (**e**).

More graphene is likely to exist at the edge of the grinding mark; further observations using SEM are shown in Figure 10. A bright spot in Figure 10a has been selected to be shown more precisely. The spot is a particle with lamellar structure with a width of about 4 μm, expected to be multilayer graphene. It was learned that particles like this are not difficult to find in Figure 10a,b, which indicates that there is a considerable amount of graphene on the edge of the grinding mark.

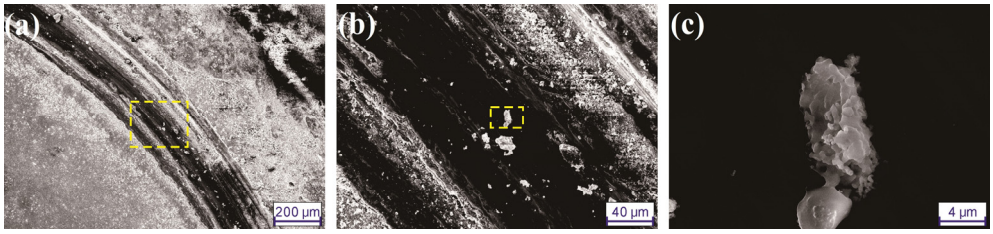

Figure 10. The gradually enlarged SEM images of the edge of the grinding mark after tribotest with G-PO: (**a**–**c**).

The true components of the particles in Figures 9 and 10 will be further tested in following studies. And if we intend to reveal the mechanism of interaction between graphene and polyphosphate and the principle that their mixtures can achieve better lubrication [32], chemical composition and distribution on the surface of the grinding mark must be made clear.

3.4. Analysis of Strengthening Mechanism of Graphene as Lubricant Additive

Two micro-areas were observed and detected using an energy dispersive spectrometer (EDS). The EDS mapping and area analytical spectrogram shown in Figure 11a,b confirmed well that the particle in Figure 9f consist of P, O, Na, Si, Ti (little), Al (little), and C, almost all the chemical elements of G-PO lubricants. The particle is an ideal hybrid of nearly all the components in G-PO. The polyphosphate adheres well to the sliding surface due to its interfacial reaction at elevated temperature with the steel surface [33], making most of the active ingredients remain in the grinding mark. Graphene plays a skeletal role to make the hybrid particle maintain a certain structure and size, and not to be easily damaged. Figure 11c,d are, namely, the EDS mapping and area scanning spectrum of the particle at the edge of the grinding mark in Figure 10c, confirming that the particle is mainly composed of C (graphene), Na, and P (polyphosphate). Because sliding is not severe at the edge of the wear scar, graphene and polyphosphate can more easily adhere to the steel surface. The existence of a certain amount of particles in a grinding mark like those two is sufficient to achieve an excellent lubrication effect.

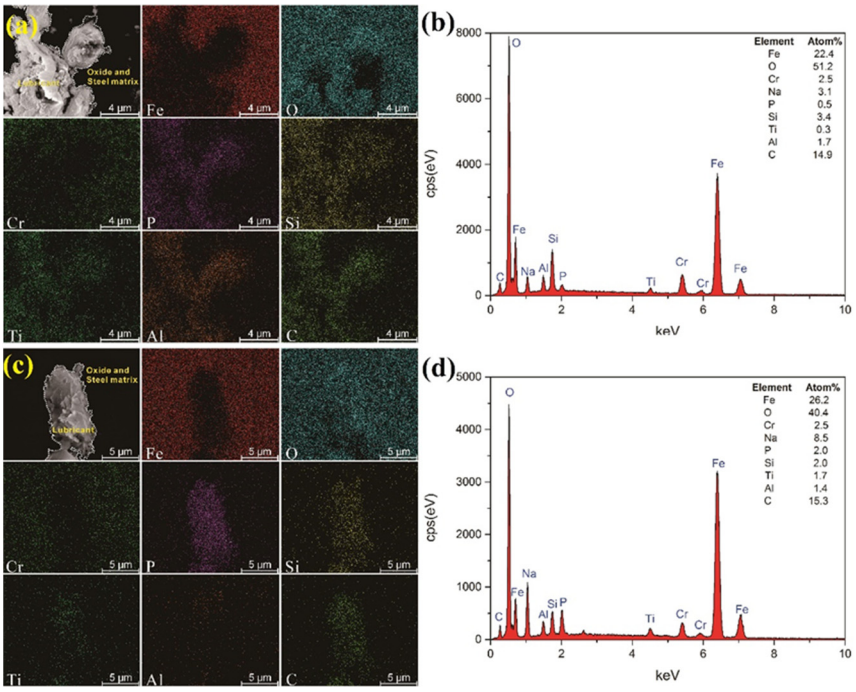

Figure 11. EDS mappings and the corresponding EDS spectra of the particle in Figure 9f (**a**,**b**) and Figure 10c (**c**,**d**).

The hybrid material is affirmed to be a kind of lubricant with excellent antifriction, anti-wear properties and durability, and it has a degree of antioxidant properties. The lubrication mechanism can be discussed by analyzing the composition and structure of the material in the grinding mark. The lubrication mechanism is preliminarily explored by means of analyzing the semi molten state of the hybrid material, showing not only the lubrication characteristics of the fluid, but also the properties of solid lubrication. The fluid part is polyphosphate, which provides viscosity for the lubricant and acts as glue to bond to graphene sheets and oxide nanopowders; the solid part is graphene and oxide nanopowders, which act, respectively, as skeletons and fillers for surface dimples. Under these two aspects, the lubricating film itself is not easily destroyed and is liable to adhere to steel surfaces. Meanwhile, according to previous studies, phosphate hybrids have a lively chemical reactivity; thus, phosphate reacts with and permeates into the iron matrix, just like firmly striking its roots into the tribological interfaces.

The lubrication mechanism of G-PO lubricant at various temperatures is figuratively described in Figure 12. At the temperature below 100 °C, all ingredients of the G-PO lubricant are dissolved or suspended in water, and the steel/steel interfaces are in a state of fluid dynamic lubrication. Phosphate dissolves in the water and increases its viscosity, and graphene and oxide nanopowder immersed in the fluid can be flexibly transferred to the position where there is a shortage of lubricating medium according to the interface condition. At this time, the three components are fragmented, with little interaction. As the temperature increases, phosphate loses moisture and its viscosity is reduced, and graphene and oxide nanopowders play major roles at this stage below 600 °C. They are prone to be extruded out of contact areas due to the pressure without phosphate adhesion. When the temperature reaches 616 °C, phosphates reach the melting point, and molten phosphates play the role of fluid lubrication. The fluid is also interspersed with graphene and oxide nanoparticles. Graphene can play the role of skeleton link at this time, so that the molten lubrication film with polyphosphates as the main body is not easy to break.

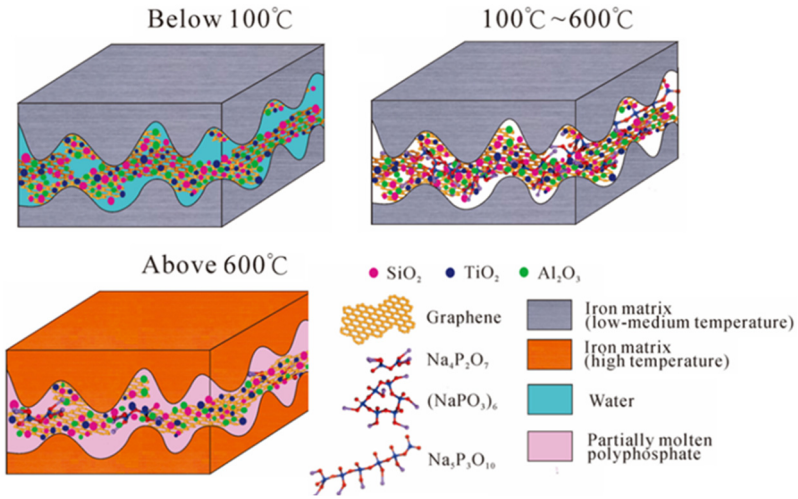

Figure 12. Lubrication mechanism of G-PO lubricant at various temperatures.

4. Conclusions

(1) Under the lubrication of the hybrid material composed of graphene, polyphosphate, and oxide nanopowders, the friction coefficient decreased by nearly 70%, and the wear reduced significantly, compared with unlubricated conditions.

(2) The strong adhesion of partially molten polyphosphate to metal surfaces, graphene sheets, and nanopowders has a positive effect on the confinement of lubricant in frictional contact areas, which greatly reduces the friction coefficient and the oxidation of the tribological interfaces.

(3) Graphene acts as a solid framework inserted in lubricants, parallel to the friction interfaces and providing excellent lateral tensile strength for lubricants. This function of graphene prevents the lubricant from breaking up, meaning that the anti-wear properties and wear resistance durability of the lubricant are guaranteed.

Author Contributions: Conceptualization, K.M. and N.K.; methodology, Q.D.; software, Q.D.; validation, X.X., Y.L. and J.W.; formal analysis, K.M.; investigation, X.X.; resources, Y.L.; data curation, J.W.; writing—original draft preparation, Q.D.; writing—review and editing, Q.D. and N.K.; visualization, Q.D.; supervision, K.M.; project administration, N.K.; funding acquisition, K.M. All authors have read and agreed to the published version of the manuscript.

Funding: This research was funded by the Field Test Project of Major Engineering Technology of China National Petroleum Corporation "Field Test of Key Equipment and Automatic Control System for Shale Gas Testing and Gas Production Integration", grant number 2022ZS05. The authors acknowledge the support of the National Natural Science Foundation of China (Grant No. 51605026).

Institutional Review Board Statement: Not applicable.

Informed Consent Statement: Not applicable.

Data Availability Statement: All relevant data are within the paper.

Conflicts of Interest: Kai-fu Mi, Xiangru Xu, Yu Lei, and Juncheng Wang are employed by the Beijing Petroleum Machinery Co., Ltd. Qingqing Ding and Ning Kong are employed by the School of Mechanical Engineering, University of Science and Technology, Beijing. Kai-fu Mi, Qingqing Ding, Xiangru Xu, Yu Lei, Juncheng Wang, and Ning Kong all have received research grants from the Beijing Petroleum Machinery Co., Ltd. The authors of the paper declare that the research was conducted in the absence of any commercial or financial relationships that could be construed as a potential conflicts of interest.

References

1. Zhao, J.; Jiang, Z. *Rolling of Advanced High Strength Steels: Theory, Simulation and Practice*; CRC Press: Boca Raton, FL, USA, 2017.
2. Zhao, J.; Jiang, Z. Thermomechanical processing of advanced high strength steels. *Prog. Mater. Sci.* **2018**, *94*, 174–242. [CrossRef]
3. Yu, X.; Jiang, Z.; Zhao, J.; Wei, D.; Zhou, J.; Zhou, C.; Huang, Q. The role of oxide-scale microtexture on tribological behaviour in the nanoparticle lubrication of hot rolling. *Tribol. Int.* **2016**, *93*, 190–201. [CrossRef]
4. Wu, H.; Zhao, J.; Xia, W.; Cheng, X.; He, A.; Yun, J.H.; Wang, L.; Huang, H.; Jiao, S.; Huang, L.; et al. Analysis of TiO2 nano-additive water based lubricants in hot rolling of microalloyed steel. *J. Manuf. Process* **2017**, *27*, 26–36. [CrossRef]
5. Wu, H.; Zhao, J.; Luo, L.; Huang, S.; Wang, L.; Zhang, S.; Jiao, S.; Huang, H.; Jiang, Z. Performance evaluation and lubrication mechanism of water-based nanolubricants containing nano-TiO_2 in hot steel rolling. *Lubricants* **2018**, *6*, 57. [CrossRef]
6. Li, M.; Yu, T.; Zhang, R.; Yang, R.; Li, H.; Wang, W. MQL milling of TC4 alloy by dispersing graphene into vegetable oil-based cutting fluid. *Int. J. Adv. Manuf. Technol.* **2018**, *99*, 1735. [CrossRef]
7. Wang, W.; Xie, Z.L.; Qu, Y.; Chang, W.; Peng, Y.; Jin, J.; Wang, K. Graphene/SiO_2 nanocomposite as water-based lubrication Tribological properties of additives. *Chin. J. Mater. Res.* **2023**, *37*, 544.
8. Ibrahim, A.M.M.; Li, W.; Xiao, H.; Zeng, Z.; Ren, Y.; Alsoufi, M.S. Energy conservation and environmental sustainability during grinding operation of Ti-6Al-4V alloys via eco-friendly oil/graphene nano additive and Minimum quantity lubrication. *Tribol. Int.* **2020**, *150*, 106387. [CrossRef]
9. Berman, D.; Deshmukh, S.A.; Sankaranarayanan, S.K.R.S.; Erdemir, A.; Sumant, A.V. Extraordinary Macroscale Wear Resistance of One Atom Thick Graphene Layer. *Adv. Funct. Mater.* **2014**, *24*, 6640–6646. [CrossRef]
10. Fu, T.; Ma, S.; Zhou, F.; Zhang, Y.; Wei, Q. Progress of functionalized graphene nanomaterials and their applications as water-based lubricating additives. *Tribology* **2022**, *42*, 408.
11. Wang, Y.; Hu, Y.; Zhao, H.; Li, J.; Wang, C.; Mao, J.; Wang, L.; Xue, Q. Research progress of graphene as additives of water-based lubricants. *Mater. Rev.* **2021**, *35*, 19055.
12. Lee, H.; Lee, N.; Seo, Y.; Eom, J.; Lee, S. Comparison of frictional forces on graphene and graphite. *Nanotechnology* **2009**, *20*, 325701. [CrossRef]
13. Ren, X.M.; Wang, Y.; He, T. Key processes and mechanism for preparing graphene by hummers method. *J. Mater. Eng.* **2013**, *1*, 1–5.
14. Roksana, M.; Monika, K.; Lukasz, S.; Noel, D.; Grażyna, G. Oxidation of graphite by different modified Hummers methods. *New Carbon Mater.* **2017**, *32*, 15–20.
15. Cui, S.G.; Zhu, H.T.; Tieu, K.; Deng, G. Insights into the behavior of polyphosphate lubricant in hot rolling of mild steel. *Wear* **2019**, *426*, 433–442. [CrossRef]

16. Kong, N. Lubrication Mechanics of Inorganic Polyphosphate in Ferrite Strip Rolling of Interstitial Free Steel. Doctoral Thesis, University of Wollongong, Wollongong, Australia, 2014.
17. Sagil, J.; Mehrshad, M. Study on High-Speed Machining of 2219 Aluminum Utilizing Nanoparticle-Enhanced Minimum Quantity Lubrication (MQL) Technique. *Surfaces* **2023**, *6*, 29–39. [CrossRef]
18. Kong, N.; Zhang, J.; Zhang, J.; Li, H.; Wei, B.; Li, D.; Zhu, H. Chemical and mechanical-induced lubrication mechanisms during hot rolling of titanium alloys using a mixed graphene-incorporating lubricant. *Nanomaterials* **2020**, *10*, 665. [CrossRef]
19. Gu, Y.; Zhao, X.; Liu, Y.; Lv, Y. Preparation and Tribological Properties of Dual-Coated TiO_2 Nanoparticles as Water-Based Lubricant Additives. *J. Nanomater.* **2014**, *2014*, 785680. [CrossRef]
20. Righi, M.C.; Loehlé, S.; De Barros Bouchet, M.I.; Mambingo-Doumbe, S.; Martin, J.M. A comparative study on the functionality of S- and P-based lubricant additives by combined first principles and experimental analysis. *RSC Adv.* **2016**, *6*, 47753–47760. [CrossRef]
21. Pu, J.B.; Wang, L.P.; Xue, Q.J. Progress of tribology of graphene and graphene-based composite lubricating materials. *Tribology* **2014**, *34*, 93–112.
22. Berman, D.; Erdemir, A.; Sumant, A.V. Reduced wear and friction enabled by graphene layers on sliding steel surfaces in dry nitrogen. *Carbon* **2013**, *59*, 167–175. [CrossRef]
23. Zhang, X.S.; Wu, Z.; Zhang, J.C. Calculation of contact stress in mechanical components. *Machinery* **2000**, *27*, 24–26.
24. Riedo, E.; Chevrier, J.; Comin, F.; Brune, H. Nanotribology of carbon based thin films: The influence of film structure and surface morphology. *Surf. Sci.* **2001**, *477*, 25–34. [CrossRef]
25. Lee, C.; Li, Q.; Kalb, W.; Liu, X.-Z.; Berger, H.; Carpick, R.; Hone, J. Frictional Characteristics of Atomically Thin Sheets. *Science* **2010**, *328*, 76–80. [CrossRef] [PubMed]
26. Berman, D.; Erdemir, A.; Sumant, A.V. Few layer graphene to reduce wear and friction on sliding steel surfaces. *Carbon* **2013**, *54*, 454–459. [CrossRef]
27. Derjaguin, B.V.; Muller, V.M.; Toporov, Y.P. Effect of contact deformations on the adhesion of particles. *J. Colloid Interface Sci.* **1975**, *53*, 314–326. [CrossRef]
28. Bhushan, B.; Sundararajan, S. Micro/nanoscale friction and wear mechanisms of thin films using atomic force and friction force microscopy. *Acta Mater.* **1998**, *46*, 3793–3804. [CrossRef]
29. Tieu, A.K.; Kong, N.; Wan, S.; Zhu, H.; Zhu, Q.; Mitchell, D.R.G.; Kong, C. The Influence of Alkali Metal Polyphosphate on the Tribological Properties of Heavily Loaded Steel on Steel Contacts at Elevated Temperatures. *Adv. Mater. Interfaces* **2015**, *2*, 1500032. [CrossRef]
30. Dresselhaus, M.S.; Jorio, A.; Hofmann, M.; Dresselhaus, G.; Saito, R. Perspectives on carbon nanotubes and graphene Raman spectroscopy. *Nano Lett.* **2010**, *10*, 751–758. [CrossRef]
31. Shin, Y.J.; Stromberg, R.; Nay, R.; Huang, H.; Wee, A.T.S.; Yang, H.; Bhatia, C.S. Frictional characteristics of exfoliated and epitaxial graphene. *Carbon* **2012**, *49*, 4070–4073. [CrossRef]
32. Khare, V.; Pham, M.Q.; Kumari, N.; Yoon, H.-S.; Kim, C.-S.; Park, J.-I.L.; Ahn, S.-H. Graphene-ionic liquid based hybrid nanomaterials as novel lubricant for low friction and wear. *Appl. Mater. Interfaces* **2013**, *5*, 4063–4075. [CrossRef]
33. Kong, N.; Tieu, A.K.; Zhu, Q.; Zhu, H.; Wan, S.; Charlie, K. Tribofilms generated from bulk polyphosphate glasses at elevated temperatures. *Wear* **2015**, *330-331*, 230–238. [CrossRef]